RESEARCH ARTICLE

Oxidative metabolism of the mycotoxins alternariol and alternariol-9-methyl ether in precision-cut rat liver slices in vitro

Britta Burkhardt[1], Judith Wittenauer[1], Erika Pfeiffer[1], Ute M. D. Schauer[2] and Manfred Metzler[1]

[1] Institute of Applied Biosciences, Chair of Food Chemistry, Karlsruhe Institute of Technology (KIT), Karlsruhe, Germany
[2] Institute of Toxicology, University of Würzburg, Würzburg, Germany

Received: September 30, 2010
Revised: January 10, 2011
Accepted: January 11, 2011

Scope: Monohydroxylation of alternariol (AOH) and alternariol-9-methyl ether (AME) has previously been reported as a prominent metabolic route under cell-free conditions. This pathway gives rise to several catechol metabolites and may therefore be of toxicological relevance.
Methods and results: To clarify whether hydroxylation of AOH and AME occurs under in vivo-like conditions in the presence of conjugation reactions, the metabolism of the *Alternaria* toxins has now been studied in precision-cut rat liver slices. Four catechol metabolites of AOH and two of AME, together with several of their *O*-methylation products, as catalyzed by catechol-*O*-methyl transferase, were clearly identified after incubation of the liver slices with AOH and AME. These metabolites were predominantly present as conjugates with glucuronic acid and/or sulfate. In preliminary studies with bile duct-cannulated male rats dosed with AOH by gavage, the four monohydroxylated metabolites of AOH could also be demonstrated in the bile either as catechols or as *O*-methyl ethers.
Conclusion: These experiments clearly show that AOH and AME undergo catechol formation in vivo and warrant closer examination of the toxicological significance of this metabolic pathway.

Keywords:
Alternariol / Alternariol methyl ether / Catechols / Oxidative metabolism / Precision-cut rat liver slices

1 Introduction

Fungi of the genus *Alternaria* are ubiquitous in areas with temperate climate and infest various crops used for human food and animal feed. Several mycotoxins produced by *Alternaria* fungi have been identified, including alternariol (AOH) and alternariol-9-methyl ether (AME; chemical structures in Fig. 1). These toxins are frequently detected in food items, e.g. wheat and other grains, apples, raspberries, tomatoes, olives, wine, apple juice and other fruit beverages [1–3].

It has been suggested that consumption of food infested by *Alternaria* fungi may be associated with an increased incidence of esophageal cancer in certain areas of China [4]. Recent studies have shown that AOH and AME are able to induce DNA strand breaks, micronuclei and gene mutations in various cultured mammalian cells [5–7], and to inhibit topoisomerase I and IIα under cell-free conditions [8]. Moreover, AOH and AME are prone to cytochrome P450 (CYP)-mediated hydroxylation in vitro, leading to catechol and hydroquinone metabolites [9]. These phase I metabolites may be of toxicological relevance because they can form reactive semiquinones and quinones. The catechol metabolites of AOH and AME were found to be *O*-methylated by catechol-*O*-methyl transferase (COMT) under cell-free

Correspondence: Professor Manfred Metzler, Institute of Applied Biosciences, Chair of Food Chemistry, Karlsruhe Institute of Technology (KIT), Adenauerring 20a, 76131 Karlruhe, Germany
E-mail: manfred.metzler@kit.edu
Fax: +49-721-608-47255

Abbreviations: AME, alternariol-9-methyl ether; **AOH,** alternariol; **COMT,** catechol-*O*-methyl transferase; **CYP,** cytochrome P450; **HO,** hydroxy; **MP,** *O*-methylation product; **NADPH,** β-nicotinamide adenine dinucleotide phosphate, reduced form; **SAM,** *S*-adenosyl-L-methionine; **TMS,** trimethylsilyl

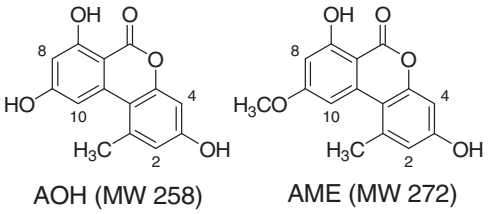

Figure 1. Chemical structures of AOH and AME. Numbered carbon atoms are sites of enzymatic hydroxylation.

conditions [9]. Our laboratory has also reported that AOH and AME are readily glucuronidated in hepatic and extrahepatic microsomes of rats, pigs and humans [10], and the formation of glucuronides and sulfates of AOH and AME has been demonstrated in cultured human Caco-2 cells [11].

As AOH and AME are targets for oxidative as well as conjugative metabolism, the aim of the present study was to investigate the fate of these compounds in an in vivo-like situation, where enzymes of both phase I and phase II metabolism are active. For this purpose, precision-cut rat liver slices were used, which are an established model for metabolic studies under in vivo-like conditions [12, 13]. A major benefit of this system is that all cell types are present and the intact tissue architecture is preserved. Cultured tissue slices are viable up to 72 h and maintain their metabolic activity during the whole time period. The present study demonstrates the formation of hydroxylated metabolites of AOH and AME and their respective *O*-methylation products (MPs) in precision-cut liver slices of male Sprague Dawley rats, indicating that oxidative metabolism occurs despite the presence of conjugation reactions. These findings were confirmed in an in vivo experiment with bile duct-cannulated rats, in which hydroxylated metabolites of AOH and their MPs were detected in the bile after administration of the mycotoxin by gavage.

2 Materials and methods

2.1 Chemicals

AOH was chemically synthesized in the laboratory of J. Podlech, Karlsruhe Institute of Technology (Karlsruhe, Germany), as previously reported [14] and contained 1.1% AME as determined by HPLC. AME was purchased by Sigma/Aldrich/Fluka (Taufkirchen, Germany) and had a purity of >96% according to HPLC analysis, containing 2.2% AOH. HPLC grade and LC-MS grade ACN and methanol were obtained from Carl Roth (Karlsruhe, Germany). Graphislactone A was kindly provided by J. Podlech. Fetal calf serum (FCS) was purchased from Invitrogen (Karlsruhe, Germany). Gentamicin, *S*-adenosyl-L-methionine (SAM), β-glucuronidase type B-1 from bovine liver, sulfatase from *Aerobacter aerogenes*, Waymouth MB 752/1 medium and all other chemicals and reagents were obtained from Sigma/Aldrich/Fluka.

2.2 Biological materials and animals

Microsomes and cytosol were prepared from the fresh liver of male untreated Wistar rats as described previously [9]. Protein contents were measured according to the method of Bradford [15], with bovine serum albumin as standard. Male Sprague Dawley rats were purchased from Harlan-Winkelmann (Borchen, Germany). Animals were kept under a 12-h dark/light cycle with free access to commercial animal feed and water.

2.3 Preparation of hydroxylated metabolites and methylation products

Oxidative metabolites of AOH and AME were generated by incubation with NADPH (β-nicotinamide adenine dinucleotide phosphate (reduced form))-fortified rat liver microsomes and extracted from the incubations with ethyl acetate as previously described [9]. The extract was evaporated to dryness and the residue dissolved in methanol for fractionation by HPLC. A Beckman system (Beckman Coulter, Brea, CA, USA) equipped with a binary pump, a DAD and 32 Karat 7.0 software for data collection and analysis was used. Separation was carried out on a 250 × 4.6 mm id, 5 µm, reversed-phase Luna C8 column (Phenomenex, Torrance, CA, USA). Solvent A was deionized water adjusted to pH 3 with formic acid and solvent B was ACN. A linear solvent gradient was started 2 min after injection, changing from 17% B to 45% in 10 min, then to 50% B in 10 min, then to 100% B in 5 min. After eluting the column with 100% B for 5 min, the initial 17% B were reached in 3 min. The flow rate was 1 mL/min and the detection wavelength 254 nm. Fractions containing hydroxylated AOH and AME metabolites were extracted with ethyl acetate and the extracts evaporated to dryness, dissolved in 50 µL methanol and used for incubations with COMT and analysis by LC-DAD-MS^n or GC-MS^2.

Purified catechol metabolites of AOH and AME were dissolved in 5 µL DMSO (final concentration 0.5%) and incubated with rat liver cytosol containing COMT and fortified with SAM as described [9]. The parent catechol metabolites and their methylation products were again extracted with ethyl acetate, fractionated by HPLC and analyzed by LC-DAD-MS^n and GC-MS^2.

2.4 Preparation and incubation of precision-cut rat liver slices

Slices with a diameter of 8 mm, a thickness of 200 µm and a wet weight between 15 and 25 mg were prepared from the livers of three male Sprague Dawley rats using a Vitron Tissue Slicer (Vitron, Tucson, AZ, USA) as reported before [16]. For each incubation, one fresh slice was placed on a stainless steel mesh half cylinder in a 20-mL glass scintillation vial containing 1.7 mL of Waymouth's MB 752/1 medium supplemented with 10% fetal calf serum and

50 μg/mL gentamicin. After 1 h at 37°C in the oxygenated atmosphere of a dynamic roller culture incubator, the insert with the slice was transferred to another vial containing 1.7 mL of medium with 50, 100 or 200 μM AOH or AME. Incubation was then continued for 24 h. During the whole time period, both surfaces of the slice were alternately exposed to gas and liquid phase, ensuring optimum supply with oxygen and nutrients. After incubation, the slice and mesh were removed from the vial, 0.1% ascorbic acid was added to the medium, and the medium was cryopreserved with liquid nitrogen and stored at −80°C until analyzed for oxidative metabolites of AOH and AME and their MPs by LC-DAD-MS^n.

2.5 Collection of bile

Two male Sprague Dawley rats of 331 and 355 g body weight were anesthesized by inhalation of oxygen containing 5% v/v isoflurane initially and 1.5% after 20 min to sustain narcosis. The bile duct was cannulated with a flexible polyethylene tubing with 0.7 mm od and 0.36 mm id (Portex, England). Each animal received 2.2 mg of AOH, dissolved in 50 μL DMSO and 400 μL corn oil, by gavage. Bile was collected in 30 min fractions, which had a volume of about 450 μL, from 0.5 h before until 4.5 h after dosing and stored at −80°C. The animal experiment was conducted at the Institute of Toxicology of the University of Würzburg under the guidelines of the German animal welfare act, and approved by a Government Review Board of the State of Bavaria (File reference 54-2531.01-59/05).

2.6 Enzymatic hydrolysis of conjugated metabolites

To determine the glucuronidated and sulfonated metabolites in tissue culture medium and bile fluid, the biological samples were mixed with an equal or a fivefold volume, respectively, of 0.1 M potassium phosphate buffer pH 7.1 containing 250 units/mL β-glucuronidase from bovine liver, 0.2 units/mL sulfatase from *Aerobacter aerogenes*, and 0.1% ascorbic acid. After 2 h at 37°C, the deconjugated metabolites were extracted three times with an equal volume of ethyl acetate. Unconjugated metabolites were extracted with ethyl acetate from the samples without enzymatic hydrolysis. Extracts were evaporated to dryness under a stream of nitrogen and the residues dissolved in 50 μL methanol. Detection of hydroxylated metabolites and MPs was carried out by using LC-DAD-MS^n analysis for medium samples and GC-MS^2 analysis for bile samples.

2.7 HPLC analysis with fluorescence detection

To determine the sum of free and conjugated AOH in rat bile, 50 μL aliquots of the bile samples were spiked with 2 μL of a 0.1 mM solution of AME in DMSO as an internal standard prior to enzymatic hydrolysis of conjugates and ethyl acetate extraction. The extracts were analyzed by HPLC, using a Shimadzu prominence system (Shimadzu Corporation, Kyoto, Japan) equipped with two pumps, autosampler, fluorescence detector and LC solution 1.22 software for data collection and analysis. The same column was used as described for the HPLC fractionation of oxidative metabolites (see Section 2.3). Solvent A was deionized water with 0.1% formic acid and solvent B was methanol. For the separation of AOH and AME, a linear solvent gradient was started immediately after injection, changing from 40% B to 100% B in 20 min. After 7 min of eluting the column with 100% B, the initial 40% B were reached in 2 min, followed by re-equilibration for 3 min. Flow rate was 0.8 mL/min, and the detector was set to $\lambda_{excitation}$ 330 nm/$\lambda_{emission}$ 430 nm.

2.8 LC-DAD-MS^n analysis

A LXQ Linear Ion Trap MS^n system (Thermo Fisher Scientific, Waltham, MA, USA) together with a Finnigan Surveyor HPLC system equipped with a binary pump, autosampler, DAD and Xcalibur 2.0.7 software for data collection and analysis was used. This allowed on-line analysis of ultraviolet (UV) absorption and MS. The column was the same as described for the HPLC fractionation of oxidative metabolites (see Section 2.3). Solvent A was deionized water without formic acid, and solvent B was ACN. For the separation of hydroxylated AOH or AME metabolites and the corresponding MPs, a linear solvent gradient was started 2 min after injection, changing from 40% B to 50% B in 5 min, then to 57% B in 5 min, then to 70% B in 12 min and then to 100% B in 5 min. After 3 min with 100% B, the initial 40% B were reached in 1 min, followed by re-equilibration for 2 min. The flow rate was 0.5 mL/min. The mass spectrometer was operated in the negative ESI mode. Nitrogen was used as sheath gas, auxiliary gas and sweep gas with flow rates of 40.0, 10.0 and 0.02 L/min, respectively. Spray voltage was 5.5 kV, spray current 0.05 μA, capillary voltage −1.0 V, capillary temperature 300°C and tube lens voltage −69.89 V. For MS^n analysis, CID voltage was set to 1.75 V. Hydroxylated AOH metabolites were identified using MS^2 analysis of the quasimolecular ions at m/z 273, the respective MPs and hydroxylated AME metabolites by MS^3 of m/z 287 > 272, and MPs of AME catechols by MS^3 of m/z 301 > 286.

2.9 GC-MS/MS analysis

A Finnigan GCQ capillary gas chromatograph (Thermo Finnigan, Austin, TX, USA) equipped with a 30 m × 25 mm id, 0.25 μm, 5% phenylmethyl MDN-5S fused-silica column (Supelco, Bellefonte, PA, USA) and coupled to an ion trap

detector was operated with electron impact (EI) ionization at 70 eV. Samples dissolved in methanol were evaporated to dryness, dissolved in 10 μL N,O-bis(trimethylsilyl)trifluoroacetamide, and 1 μL was injected on-column with an injection port temperature of 50°C. The column oven was programmed from 60°C (1 min hold) to 290°C (15 min hold) at a rate of 15°C/min. The transfer line and ion source were kept at 275°C and 200°C, respectively. Helium was used as carrier gas with a flow rate of 40 cm/s. Detection of AOH metabolites was carried out by using the dual-MS/MS mode (cap voltage 1.7 V for 0.15 min) on [M-CH_3] ions of AOH catechols (*m/z* 547) and MPs (*m/z* 489), and the product ions were scanned from *m/z* 50–600.

3 Results and discussion

3.1 Preparation of reference compounds

For the identification of AOH and AME metabolites in rat liver slices and rat bile, reference compounds were required. Previous studies with NADPH-fortified liver microsomes have shown that AOH and AME are monohydroxylated at four positions (Fig. 1), giving rise to metabolites with catechol and/or hydroquinone structures [9]. In intact cells, *O*-methylation of catechols is catalyzed by COMT. For each hydroxylated AOH and AME metabolite with catechol structure, the formation of two MPs is possible, which is exemplified for 2-hydroxy-AOH (2-HO-AOH) in Fig. 2.

The monohydroxylated metabolites of AOH and AME were obtained by incubation of the parent mycotoxins with NADPH-fortified rat liver microsomes and identified according to our previous study [9]. The hydroxylation products were fractionated by HPLC and the isolated metabolites incubated with SAM-fortified rat liver cytosol containing COMT. LC-DAD-MS^n analysis of the reaction products showed that each catechol gave rise to one or two new compounds, which were not present in control incubations without SAM (Table 1). The new products had ultraviolet spectra similar to those of AOH and AME (data not shown), and exhibited [M-H] ions of the respective MPs (*m/z* 287 with AOH and *m/z* 301 with AME) in their mass spectra obtained with negative ESI.

The ESI-MS^n data of the hydroxylated AOH and AME metabolites and their MPs are listed in Table 2. The mass spectra of all compounds exhibited [M-H] ions with virtually 100% intensity. The catechol metabolites of AOH showed differences in the daughter ion spectra (MS^2) of the [M-H] ion. In contrast, all their MPs gave rise to only one fragment ion at *m/z* 272 upon MS^2 of the [M-H] ion, corresponding to the loss of a methyl group, but differed in MS^3. However, these differences could not be used to elucidate their exact chemical structure, i.e. the position of the *O*-methyl group. The MPs of all HO-AMEs exhibited a quantitative loss of one *O*-methyl group at MS^2 and of the second *O*-methyl group at MS^3 and could not be distinguished at this MS level (Table 2).

Although the mass spectra did not clarify the exact structures of the MPs, the chromatographic properties of some MPs helped with their tentative identification. For example, the MP of 8-HO-AOH may carry the *O*-methyl group either at C-7 or C-8 or C-9. *O*-Methylation at C-7 would disrupt the hydrogen bonding with the keto group at C-6 and lead to a marked increase in polarity, as has been noted for glucuronides of AOH conjugated at this site [10], whereas *O*-methylation at C-9 would yield a MP identical with 8-HO-AME. Since neither of such products were observed, the MP of 8-HO-AOH is suggested to have the structure of 8-methoxy-AOH (Table 1). 10-HO-AOH may be *O*-methylated at C-9 or C-10; since the MP has the same LC retention time and MS^3 mass spectrum as 10-HO-AME, the methyl group must be attached to the hydroxyl group at C-9 (Table 1). Of the two MPs of 4-HO-AME, one must be *O*-methylated at C-3 and the other one at C-4; since MP-1 cochromatographed with the reference compound graphislactone A, which is 3-*O*-methyl-4-HO-AOH, MP-2 must be 4-methoxy-AME (Table 1). Finally, the striking difference in LC retention time of the two MPs of 8-HO-AME implied that the more polar MP-1 is *O*-methylated at C-7 because of the disrupted hydrogen bonding (see above), leaving the structure of 8-methoxy-AME for MP-2 (Table 1).

The LC retention times in combination with the mass spectra at different MS^n levels allowed the LC-MS analysis of mixtures of the hydroxylated metabolites of AOH and AME and their MPs (Fig. 3). This method was therefore used for the analysis of rat liver slices (see Section 3.2).

3.2 Metabolism of AOH and AME in precision-cut rat liver slices

Precision-cut liver slices of male Sprague Dawley rats were incubated at 37°C in the oxygenated atmosphere of a rotat-

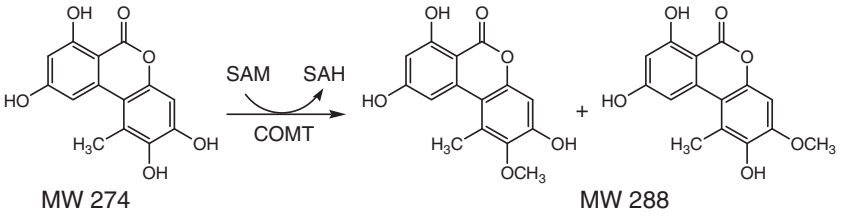

Figure 2. Scheme of COMT-catalyzed *O*-methylation of 2-HO-AOH. SAH, *S*-adenosyl-L-homocysteine.

Table 1. Chromatographic properties of oxidative AOH and AME metabolites and their MPs

Oxidative metabolite	Retention time (min)		MP	Retention time (min)		Position of methyl group	Ratio[a)] of MP-1/MP-2
	LC	GC[b)]		LC	GC[b)]		
2-HO-AOH	11.8	27.2	MP-1	13.1	25.3	C-2 or C-3[c)]	6:1
			MP-2	14.2	27.0		
4-HO-AOH	10.5	23.7	MP-1	12.1	23.6	C-3 or C-4[c)]	1:12
			MP-2	12.6	24.3		
8-HO-AOH	9.5	25.0	MP	12.7	24.7	C-8[d)]	–
10-HO-AOH	11.3	21.4	MP	13.9	21.2	C-9[e)]	–
2-HO-AME	16.8	27.5	MP-1	20.3	25.4	C-2 or C-3[c)]	1:1
			MP-2	21.8	27.3		
4-HO-AME	14.9	23.6	MP-1	18.8	23.6	C-3[f)]	1:7
			MP-2	19.8	24.3	C-4	
8-HO-AME	11.2	26.0	MP-1	9.5	26.5	C-7[g)]	1:5
			MP-2	16.7	25.6	C-8	
10-HO-AME[h)]	13.9	21.2	–	–	–	–	–

a) According to UV absorbance at 254 nm.
b) TMS derivatives.
c) MPs not distinguishable by GC-MS^2 analysis.
d) Tentative location of methyl group by exclusion.
e) Identical LC retention time and LC-MS^2 data with 10-HO-AME.
f) This MP has identical retention times and MS/MS data with graphislactone A in LC-MS and GC-MS.
g) This MP has a higher polarity than 8-HO-AME, suggesting methylation at C-7.
h) No reaction with COMT because of hydroquinone structure.

Table 2. ESI-mass spectra of monohydroxylated AOH and AME metabolites and their MPs

Metabolite		**MS^2 of M-H (*m/z* 273)**
2-HO-AOH		273 (100), 258 (10), 229 (19)
4-HO-AOH		273 (29), 258 (100), 229 (13)
8-HO-AOH		273 (100)
10-HO-AOH		273 (100), 258 (63), 245 (26), 229 (18), 217 (33), 201 (33)
		MS^3 of M-H (*m/z* 287 > *m/z* 272)
2-HO-AOH	MP-1	271 (100), 257 (26), 244 (76), 243 (19), 200 (44)
	MP-2	272 (12), 271 (100), 257 (28), 244 (73), 243 (17), 200 (46)
4-HO-AOH	MP-1	271 (11), 257 (24), 244 (10), 243 (14), 216 (48), 188 (100)
	MP-2	257 (22), 244 (12), 243 (16), 216 (46), 188 (100)
8-HO-AOH	MP	272 (100), 244 (59)
10-HO-AOH	MP	272 (20), 257 (100)
2-HO-AME		272 (15), 271 (100), 257 (30), 244 (75), 243 (21), 200 (51)
4-HO-AME		257 (21), 243 (13), 216 (47), 188 (100)
8-HO-AME		272 (100), 244 (14)
10-HO-AME		272 (20), 257 (100)
		MS^3 of M-H (*m/z* 301 > *m/z* 286)
HO-AME	MP	271 (100)

Numbers in parentheses indicate % relative intensity. Only intensities ≥10% are given.

ing incubator. Each vial contained one liver slice on a mesh surface and tissue culture medium with the respective mycotoxin at concentrations of 50, 100 or 200 μM. Each incubation was carried out in triplicate with slices originating from one animal. Altogether, the liver slices of three animals were used.

Rat liver slices were incubated with 50 μM AOH or AME for 24 h. Half of the incubation medium was then directly extracted with ethyl acetate and the extract analyzed with LC-DAD-MS^n to determine the unconjugated oxidative metabolites and MPs. In the other half of the medium, glucuronides and sulfates were hydrolyzed prior to extraction, thereby obtaining the sum of free and conjugated metabolites. The pattern of metabolites detected is listed in Table 3. Conjugates represented 86% of the total AOH metabolites and 74% of the AME metabolites. Several hydroxylation products of AOH and AME were detectable both as catechol metabolites and their MPs, clearly showing that aromatic hydroxylation of both *Alternaria* toxins took place under these in vivo-like conditions in the presence of conjugation reactions.

Significant differences were noted between AOH and AME with respect to the pattern of metabolites and the extent of oxidative metabolism. Hydroxylation at C-2 predominated with AOH, whereas hydroxylation at C-8 was preferred with AME (Table 3). 8-HO-AME was also the major hydroxylation product of AME with rat liver microsomes [9]. In contrast, the preferential hydroxylation of

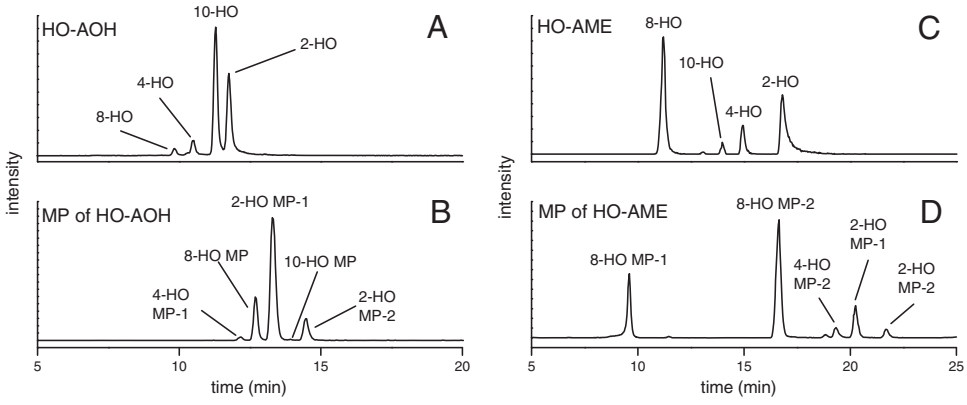

Figure 3. LC-MS profiles (TIC) of mixtures of hydroxylated metabolites of AOH (A) and AME (C) as well as the respective MPs of HO-AOH (B) and HO-AME (D). MS^n modes: HO-AOH, MS^2 of *m/z* 273; MP of HO-AOH, MS^3 of *m/z* 287 > 272; HO-AME, MS^3 of *m/z* 287 > 272; MP of HO-AME, MS^3 of *m/z* 301 > 286.

Table 3. Amounts of free and conjugated metabolites detected in the culture medium after incubation of precision-cut rat liver slices with 50 μM AOH or AME for 24 h

AOH metabolites	Free	Conjugate	AME metabolites	Free	Conjugate
2-HO-AOH	4.2 ± 7.2	17.4 ± 9.3	2-HO-AME	nd	nd
2-HO-AOH MP-1	11.1 ± 1.7	48.1 ± 4.8	2-HO-AME MP-1	nd	nd
2-HO-AOH MP-2	nd[a)]	1.0 ± 0.1	2-HO-AME MP-2	nd	nd
4-HO-AOH	nd	3.7 ± 0.4	4-HO-AME	nd	1.9 ± 0.3
4-HO-AOH MP-1	nd	0.2 ± 0.2	4-HO-AME MP-1	nd	nd
4-HO-AOH MP-2	1.0 ± 0.2	2.8 ± 0.5	4-HO-AME MP-2	4.2 ± 0.9	0.8 ± 0.5
8-HO-AOH	nd	6.7 ± 3.1	8-HO-AME	6.7 ± 4.2	24.1 ± 9.9
8-HO-AOH MP	nd	4.9 ± 4.3	8-HO-AME MP-1	nd	1.4 ± 0.6
10-HO-AOH	nd	1.3 ± 0.2	8-HO-AME MP-2	nd	2.6 ± 0.9
10-HO-AOH MP	nd	nd	10-HO-AME	nd	nd

Conjugated metabolites represent the sum of glucuronides and sulfates. Data are expressed as pmol metabolite per mg tissue and are the mean ± SD of three slices originating from one animal.
a) nd, not detectable (< 0.1).

AOH at C-2 in rat liver slices differed markedly from the hydroxylation pattern observed in microsomal incubations, where 10-HO-AOH was the major metabolite [9]. This discrepancy may be due to the poor stability of this metabolite, which has been observed in our laboratory before (data not shown). 10-HO-AOH has both catechol and hydroquinone moieties at the same aromatic ring, which make it highly susceptible to autoxidation and reaction with cellular macromolecules. Therefore, it must be expected to survive the 40-min microsomal incubation better than the 24-h incubation of liver slices. Notably, the total amount of AME metabolites detectable in liver slices was only about 40% of the total AOH metabolites, which is in contrast to the higher activity of CYP enzymes for AME as compared to AOH [17].

In further studies with rat liver slices, the concentration of the toxins was varied. Because of the poor metabolization of AME, these experiments were only done with AOH. Increase of the AOH concentration from 50 to 100 μM had no effect on the metabolic pattern and the total amount of metabolites. However, incubation with 200 μM AOH caused a decrease in the number and amount of oxidative metabolites and MPs, possibly due to toxic effects on the metabolic enzymes (data not shown).

3.3 Oxidative AOH metabolites in rat bile

Our studies with rat liver slices have shown that AOH and AME undergo CYP-mediated oxidative metabolism even in the presence of phase II enzymes. According to recent studies in the Caco-2 Millicell® system, which is a widely accepted in vitro model to assess intestinal absorption and metabolism of xenobiotic compounds, AOH must be expected to be extensively and rapidly absorbed from the intestinal lumen in vivo and to reach the portal blood both as aglycone and as glucuronide and sulfate conjugate [11]. In contrast, intestinal absorption of AME appears to be poor and sluggish [11]. To demonstrate the intestinal absorption and formation of oxidative AOH metabolites in vivo, two anesthesized and bile duct-cannulated male Sprague Dawley rats received a single dose of 2.2 mg AOH by gavage, and the bile was collected in 0.5 h fractions from 0.5 h before to 4.5 h after dosing. After enzymatic hydrolysis of the conjugates, the bile fraction assumed to contain the highest amount of AOH was analyzed for hydroxylated AOH metabolites and their MPs. As $LC\text{-}MS^n$ proved to be not sensitive enough, $GC\text{-}MS^2$ had to be used. The GC retention times of the trimethylsilyl (TMS) derivatives of hydroxylated AOH metabolites and their MPs were first determined with the

reference compounds (see Section 3.1.) and are listed in Table 1. The mass spectrometer was employed in the dual-MS^2 mode, which means that MS^2 of the molecular ions of the TMS derivatives of AOH catechols (*m/z* 547) and the respective MPs (*m/z* 489) were depicted in one chromatogram. The resulting electron impact mass spectra (Table 4) gave rise to one major fragment ion (*m/z* 459), representing the [M-88] and [M-30] ions of the catechols and MPs, respectively. The loss of 88 amu is characteristic for AOH metabolites with vicinal hydroxyl groups, whereas loss of 30 amu indicates that the hydroxyl group is located next to a methoxy group [9]. Even though distinction of the metabolites by mass spectrometry of their TMS derivatives was not possible, different GC retention times allowed identification of the hydroxylated AOH metabolites and their MPs in one analysis.

In Fig. 4, chart A depicts the GC profile of a reference mixture of hydroxylated AOH metabolites and their MPs, and chart B the resulting metabolite profile in the 1–1.5 h bile fraction of a rat dosed with AOH. Several peaks could be observed that were not present in the control bile collected prior to administration of AOH. The major peaks were 10-HO-AOH and one MP each of 2-HO-AOH and 4-HO-AOH. Furthermore, small peaks of several other AOH metabolites were detected, such as 4-HO-AOH and a MP of 8-HO-AOH (Fig. 4B). However, caution should be exerted with quantitative assessments because the sensitivity for different metabolites may vary widely due to differences in ionization. The same oxidative AOH metabolites and MPs as depicted in Fig. 4B were observed when pooled aliquots of the other bile samples of rat 1 and 2 were analyzed by GC-MS^2 (data not shown). These results clearly show that oxidative metabolites of AOH and their MPs are generated in rat liver in vivo after oral administration of AOH. Like in liver slices in vitro (see Section 3.2), all four monohydroxylation products of AOH were formed in rat liver in vivo. The pattern of in vitro and in vivo metabolites should not be compared in quantitative terms because of the differences between LC-MS and GC-MS regarding the ionization of AOH metabolites.

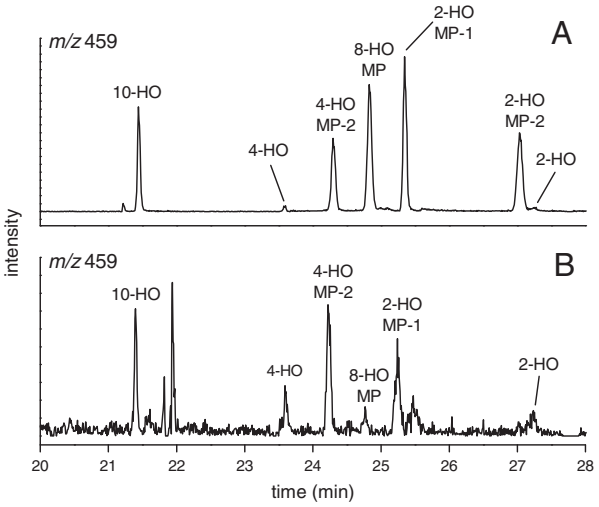

Figure 4. GC-MS^2 profile of a mixture of AOH catechols and MPs (chart A) and of the extract of rat bile after hydrolysis of glucuronides and sulfates (chart B). MS mode: dual-MS^2 of *m/z* 547 (molecular ion of trimethylsilylated HO-AOH) and *m/z* 489 (molecular ion of trimethylsilylated MPs of HO-AOH). The chromatograms are depicted as ion current at *m/z* 459, which is the [M-88] ion of hydroxylated AOH metabolites and [M-30] ion of MPs.

Table 4. EI mass spectra of the TMS derivatives of monohydroxylated AOH metabolites and their MPs

Metabolite		**MS^2 of M (*m/z* 547)**
2-HO-AOH		548 (19), 547 (100), 476 (14), 475 (43), 460 (12), 459 (45), 387 (15)
4-HO-AOH		548 (11), 547 (100), 531 (8), 476 (13), 475 (41), 459 (30)
8-HO-AOH		547 (87), 532 (35), 517 (20), 460 (13), 459 (100), 387 (14)
10-HO-AOH		547 (40), 460 (12), 459 (100)
		MS^2 of M (*m/z* 489)
2-HO-AOH	MP-1	489 (21), 459 (100)
	MP-2	459 (100)
4-HO-AOH	MP-1	489 (16), 459 (100)
	MP-2	489 (14), 459 (100)
8-HO-AOH	MP	489 (17), 459 (100)
10-HO-AOH	MP	489 (20), 459 (100)

Numbers in parentheses indicate percentage relative intensity. Only intensities ≥10% are given.

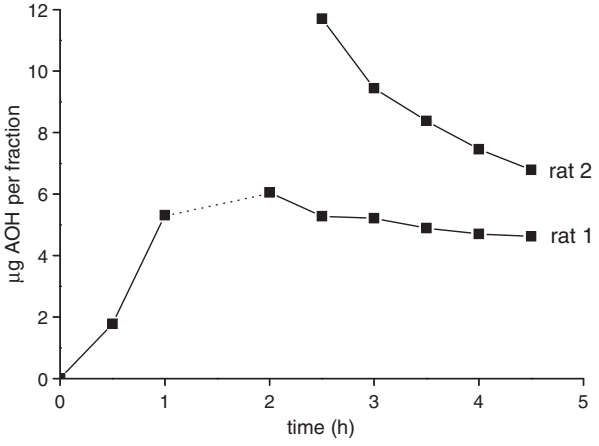

Figure 5. Amount of AOH (sum of free and conjugated compound) in the bile of two male Sprague Dawley rats dosed with AOH by gavage. AOH was quantified by HPLC with fluorescence detection. Values represent mean of three determinations for each fraction. The bile fraction of rat 1 collected between 1 and 1.5 h and the bile fractions of rat 2 excreted during the first 2 h after gavage were not available for analysis.

Aliquots of the bile samples were used to quantify the total amount of free and conjugated AOH by using HPLC with fluorescence detection and an external calibration curve with AME as internal standard. The time course of biliary AOH excretion of two rats is depicted in Fig. 5. Although not all collected bile samples were available for analysis, a rough idea about the kinetics can be derived from this study. Following a steep initial increase directly after gavage, the concentration of AOH in the bile decreased rather slowly between 2 and 4.5 h. From the AOH concentration and volume of each bile fraction, it was estimated that 2–4% of the AOH dose were excreted with the bile during the 4.5 h collection period. The low and delayed biliary excretion of AOH may indicate extensive tissue distribution of AOH, long plasma half-life, and possibly accumulation after repeated exposure. These aspects of the pharmacokinetics of AOH and also of AME should be addressed in future studies.

4 Concluding remarks

In the present study on the fate of AOH and AME in precision-cut rat liver slices, we were able to detect hydroxylated metabolites in an in vivo-like situation, where conjugation reactions are operative. The relevance of oxidative metabolism was confirmed for AOH in an in vivo experiment with rats. Together, these results show that precision-cut rat liver slices are a suitable in vitro model for metabolic studies under in vivo-like conditions. As hydroxylated AOH and AME metabolites have catechol structure, further studies will be needed to clarify the relevance of oxidative metabolism for the toxicity of these important *Alternaria* toxins.

This study was supported by KIT (Research Program "Mycotoxins" as part of the Research Initiative "Food and Health"). The authors thank Doris Honig and Sabine Jung for helping with the GC-MS analyses and preparation of reference compounds, respectively. The authors also thank Professor J. Podlech for providing AOH and graphislactone A.

The authors have declared no conflict of interest.

5 References

[1] Scott, P. M., Analysis of agricultural commodities and foods for *Alternaria* mycotoxins. *J. AOAC Int.* 2001, *84*, 1809–1817.

[2] Scott, P., Lawrence, G., Lau, B., Analysis of wines, grape juices and cranberry juices for *Alternaria* toxins. *Mycotoxin Res.* 2006, *22*, 142–147.

[3] Chełkowski, J. (Ed.), *Alternaria. Biology, Plant Diseases and Metabolites*, Elsevier, Amsterdam 1992.

[4] Liu, G. T., Qian, Y. Z., Zhang, P., Dong, W. H. et al., Etiological role of Alternaria alternata in human esophageal cancer. *Chin. Med. J. (Engl.)* 1992, *105*, 394–400.

[5] Pfeiffer, E., Eschbach, S., Metzler, M., *Alternaria* toxins: DNA strand-breaking activity in mammalian cells in vitro. *Mycotoxin Res.* 2007, *23*, 152–157.

[6] Lehmann, L., Wagner, J., Metzler, M., Estrogenic and clastogenic potential of the mycotoxin alternariol in cultured mammalian cells. *Food Chem. Toxicol.* 2006, *44*, 398–408.

[7] Brugger, E. M., Wagner, J., Schumacher, D. M., Koch, K. et al., Mutagenicity of the mycotoxin alternariol in cultured mammalian cells. *Toxicol. Lett.* 2006, *164*, 221–230.

[8] Fehr, M., Pahlke, G., Fritz, J., Christensen, M. O. et al., Alternariol acts as a topoisomerase poison, preferentially affecting the IIá isoform. *Mol. Nutr. Food Res.* 2009, *53*, 441–451.

[9] Pfeiffer, E., Schebb, N. H., Podlech, J., Metzler, M., Novel oxidative in vitro metabolites of the mycotoxins alternariol and alternariol methyl ether. *Mol. Nutr. Food Res.* 2007, *51*, 307–316.

[10] Pfeiffer, E., Schmit, C., Burkhardt, B., Altemöller, M. et al., Glucuronidation of the mycotoxins alternariol and alternariol-9-methyl ether in vitro: chemical structures of the glucuronides and activities of human UDP-glucuronosyltransferase isoforms. *Mycotoxin Res.* 2009, *25*, 3–10.

[11] Burkhardt, B., Pfeiffer, E., Metzler, M., Absorption and metabolism of the mycotoxins alternariol and alternariol-9-methyl ether in Caco-2 cells in vitro. *Mycotoxin Res.* 2009, *25*, 149–157.

[12] Parrish, A. R., Gandolfi, A. J., Brendel, K., Precision-cut tissue slices: applications in pharmacology and toxicology. *Life Sci.* 1995, *57*, 1887–1901.

[13] Ekins, S., Past, present, and future applications of precision-cut liver slices for in vitro xenobiotic metabolism. *Drug Metab. Rev.* 1996, *28*, 591–623.

[14] Koch, K., Podlech, J., Pfeiffer, E., Metzler, M., Total synthesis of alternariol. *J. Org. Chem.* 2005, *70*, 3275–3276.

[15] Bradford, M. M., A rapid and sensitive method for the quantitation of microgram quantities of protein utilizing the principle of protein-dye binding. *Anal. Biochem.* 1976, *72*, 248–254.

[16] Pfeiffer, E., Metzler, M., Effect of bisphenol A on drug metabolising enzymes in rat hepatic microsomes and precision-cut rat liver slices. *Arch. Toxicol.* 2004, *78*, 369–377.

[17] Pfeiffer, E., Burkhardt, B., Altemöller, M., Podlech, J. et al., Activities of human recombinant cytochrome P450 isoforms and human hepatic microsomes for the hydroxylation of *Alternaria* toxins. *Mycotoxin Res.* 2008, *24*, 117–123.

